ELSEVIER

Journal of Organometallic Chemistry 571 (1998) 129–138

Journal of Organometallic Chemistry

Trends in the structure and bonding of $[MCl_2\{(C_4H_3S)ECH_3\}_2]$ (M = Pd, Pt; E = Te, Se)

Raija Oilunkaniemi [a,*], Jarno Komulainen [a], Risto S. Laitinen [a], Markku Ahlgrén [b], Jouni Pursiainen [a]

[a] *Department of Chemistry, University of Oulu, PO Box 333, FIN-90571 Oulu, Finland*
[b] *Department of Chemistry, University of Joensuu, PO Box 111, FIN-90801 Joensuu, Finland*

Received 26 June 1998

Abstract

The complex formation of $(C_4H_3E)E'Me$ (E = S, O; E′ = Te, Se) (**1**–**4**) with palladium and platinum has been explored by use of NMR spectroscopy and X-ray diffraction. Whereas the ^{125}Te-NMR spectra of $[PdCl_2\{(C_4H_3E)TeMe\}_2]$ [E = S (**5**), E = O (**6**)] show the existence of both *cis*- and *trans*-isomers in solution the spectroscopic information of $[MCl_2\{(C_4H_3E)SeMe\}_2]$ (M = Pd, Pt, E = S, O; **8**–**10**) indicates the presence of only one isomer. The crystal structure determinations have shown that **5** and **6** are isomorphous and crystallize as *cis*-isomers forming dimers with close chalcogen–halogen contacts. In contrast, **8** and **10** have turned out to be *trans*-isomers and form skewed stacks that are bound together in a helical arrangement by weak hydrogen bonds. The structural data indicate that back donation may weakly contribute to the palladium–tellurium bonding in **5** and **6**. In **8** and **10** the effects of the back bonding are negligible.

Keywords: Tellurium; Selenium; Palladium complex; Platinum complex; X-ray crystallography; NMR spectroscopy

1. Introduction

Whereas the structural chemistry of palladium and platinum complexes of chalcogenoethers has seen considerable research activity in recent years [1–4], the information is rather scattered and the factors affecting the bonding and stereochemistry of the complexes are still not as well understood as those of the phosphine complexes [5]. The seleno- and telluroether complexes find potential utility as precursors for the low-temperature syntheses of binary transition metal selenides and tellurides that could have applications in the fabrication of new electronic materials [4]. The coordination chemistry of thiophene-containing transition metal complexes has also attracted attention because of their role as catalysts in the hydrodesulfuration reactions by thiophenes [6,7].

Mononuclear $[ML_2X_2]$ complexes (M = Pd, Pt; L = two organic monodentate ligands containing one selenium or tellurium donor atom each, or one didentate ligand containing two chalcogen donor atoms; X = halide) form a rather well-explored series [1–4]. Most of the experimental work involving the structural characterization, however, has been carried out in solution [8–10] and the solid state information is rather sparse [11–18]. In this work we report a detailed structural study of $[MCl_2\{(C_4H_3E)E'Me\}_2]$ (M = Pd, Pt; E = S, O; E′ = Se, Te) both in solution and in the solid state as a part of a systematic investigation on the structures, bonding, and chemical properties of the allotropes and compounds of chalcogen elements.

* Corresponding author. Fax: +358 8 5531608; e-mail: Raija.Oilunkaniemi@oulu.fi

0022-328X/98/$ - see front matter
PII S0022-328X(98)00899-7

2. Experimental

2.1. General

All synthetic work was conducted under a dry argon atmosphere. Tetrahydrofuran (THF, Aldrich) was distilled under nitrogen from Na/benzophenone. All other solvents were degassed with argon. Thiophene (Riedel de Haen) and furan (Aldrich) were distilled before use. $[PdCl_2(PhCN)_2]$ and $[PtCl_2(PhCN)_2]$ were synthesized by modifiying the method of Kharasch et al. [19].

2.2. Preparation of the ligands

Methyl(2-thienyl)tellurane (**1**), methyl(2-furyl)-tellurane (**2**) methyl(2-thienyl)selane (**3**), and methyl(2-furyl)selane (**4**) were prepared using the modified procedure of Engman and Cava [20]. The preparation is exemplified in detail for **1** below.

n-Butyllithium (5 ml, 12.5 mmol, 2.5 M solution in hexanes, Aldrich) was added into 40 ml of a dry, ice-cooled THF solution of thiophene (1 ml, 12.7 mmol) with stirring. The ice bath was removed and the solution was further stirred for 1 h. Freshly ground elemental tellurium (1.59 g, 12.4 mmol, Cerac) was rapidly added and the stirring was continued for 2 h until all tellurium was completely dissolved. Upon the addition of methyl iodide (1 ml, 16 mmol) the color of the solution turned pale yellow. The reaction mixture was poured into water and extracted several times with diethyl ether. The combined organic layers were dried with $MgSO_4$. Evaporation of the solvent afforded a yellow oil (yield 2.16 g, 77%). The product was not further purified (MS: M^+ 228 as required for **1**).

The ligands **2**–**4** were prepared in a similar fashion. The yields and the m/z for the molecular ions are the following: $(C_4H_3O)TeMe$ (**2**) (38%; M^+ 212), $(C_4H_3S)SeMe$ (**3**) (62%; M^+ 178), and $(C_4H_3O)SeMe$ (**4**) (41%; M^+ 162).

2.3. Preparation of $[MCl_2\{(C_4H_3E)E'Me\}_2]$ ($M = Pd$, Pt; $E = O$, S, $E' = Se$, Te) (**5**–**10**)

Dichlorobis{methyl(2-thienyl)tellurane}palladium(II) (**5**) was prepared by adding a solution of methyl(2-thienyl)tellurane (0.30 g, 1.4 mmol) in 10 ml of dichloromethane into 30 ml of a dichloromethane solution of $[PdCl_2(PhCN)_2]$ (0.213 g, 0.6 mmol) and stirred overnight. An orange–red precipitate was separated by filtration. The precipitation was completed by addition of hexane to the filtrate The precipitates were combined and washed with hexane and diethylether. The recrystallization from chloroform afforded 0.250 g (yield 66%) of orange–red tabular crystals of $[PdCl_2\{(C_4H_3S)TeMe\}_2]$. Anal. Calc. for $C_{10}H_{12}Cl_2PdS_2Te_2$: C 19.10; H 1.92; S 10.20. Found: C 19.65; H 1.87; S 10.03. M.p. (decomposition) 136–138°C.

All other complexes (**6**–**10**) were prepared in a similar fashion except that for the syntheses of the selenium-containing species, acetone was used as a solvent in place of dichloromethane.

2.3.1. $[PdCl_2\{(C_4H_3O)TeMe\}_2]$ (**6**)

Brown–red tabular crystals (yield 50%). Anal. Calc. for $C_{10}H_{12}Cl_2PdO_2Te_2$: C 19.39 H 2.32. Found: C 20.06 H 2.36. M.p. (decomposition) 138–140°C.

2.3.2. $[PtCl_2\{(C_4H_3S)TeMe\}_2]$ (**7**)

Brown–red microcrystalline material (yield 53%). Anal. Calc. for $C_{10}H_{12}Cl_2PtS_2Te_2$: C 16.53 H 1.73 S 8.51. Found: C 16.74 H 1.69 S 8.94. M.p. (decomposition) 140–142°C.

2.3.3. $[PdCl_2\{(C_4H_3S)SeMe\}_2]$ (**8**)

Orange needle-like crystals (yield 68%). Anal. Calc. for $C_{10}H_{12}Cl_2PdS_2Se_2$: C 22.90 H 2.01 S 11.94. Found: C 22.60 H 2.28 S 12.06. M.p. (decomposition) 144–145°C.

2.3.4. $[PdCl_2\{(C_4H_3O)SeMe\}_2]$ (**9**)

Orange microcrystalline material (yield 56%). Anal. Calc. for $C_{10}H_{12}Cl_2PdO_2Se_2$: C 24.05 H 2.42. Found: C 25.60 H 2.76. M.p. (decomposition) 143–145°C.

2.3.5. $[PtCl_2\{(C_4H_3S)SeMe\}_2]$ (**10**)

Yellow needle-like crystals (yield 60%). Anal. Calc. for $C_{10}H_{12}Cl_2PtS_2Se_2$: C 20.03 H 1.99 S 10.37. Found: C 19.37 H 1.95 S 10.34. M.p. (decomposition) 162–163°C.

2.4. NMR spectroscopy

The NMR spectra were recorded on a Bruker DPX400 spectrometer operating at 100.61, 76.31, and 126.24 MHz for ^{13}C, ^{77}Se and ^{125}Te, respectively. The spectral widths were 20.161, 114.943, and 126.582 kHz for ^{13}C, ^{77}Se, and ^{125}Te, respectively. The respective pulse widths were 5.0, 7.0, and 6.0 μs. The pulse delay for carbon was 3.0 s, for selenium 1.6 s, and for tellurium 1.6 s. The ^{13}C accumulations contained ca. 30000 transients, and the ^{77}Se and the ^{125}Te accumulations ca. 50000 transients each. Tetramethylsilane was used as an internal standard for ^{13}C chemical shifts. The saturated solutions of H_6TeO_6 (aq) and SeO_2 (aq) were used as external standards for ^{77}Se and ^{125}Te chemical shifts. All spectra were recorded in $CDCl_3$ that served as an internal ^2H lock. Chemical shifts (ppm) are reported relative to Me_4Si, and to neat Me_2Se and Me_2Te [$\delta(Me_2Se) = \delta(SeO_2) + 1302$; $\delta(Me_2Te) = \delta(H_6TeO_6) + 712$].

Table 1
Details of the structure determination of *cis*-[$PdCl_2\{(C_4H_3S)TeCH_3\}_2$] (**5**), *cis*-[$PdCl_2\{(C_4H_3O)TeCH_3\}_2$] (**6**), *trans*-[$PdCl_2\{(C_4H_3S)SeCH_3\}_2$], (**8**) and *trans*-[$PtCl_2\{(C_4H_3S)SeCH_3\}_2$] (**10**)[a]

	5	**6**	**8**	**10**
Crystal data				
Compound	[$PdCl_2\{(C_4H_3S)TeCH_3\}_2$]	[$PdCl_2\{(C_4H_3O)TeCH_3\}_2$]	[$PdCl_2\{(C_4H_3S)SeCH_3\}_2$]	[$PtCl_2\{(C_4H_3S)SeCH_3\}_2$]
Relative molecular mass	628.8	596.7	531.5	620.2
Crystal system	Monoclinic	Monoclinic	Monoclinic	Monoclinic
Space group	$C2/c$	$C2/c$	$P2_1/c$	$P2_1/c$
a (Å)	23.689(4)	23.268(1)	7.600(2)	7.663(2)
b (Å)	14.241(3)	13.836(1)	5.789(1)	5.770(1)
c (Å)	10.802(2)	10.663(1)	17.855(4)	17.826(4)
β (°)	114.26(1)	115.05(1)	95.80(3)	96.30(2)
V (Å^3)	3322.3(11)	3109.9(4)	781.5(3)	783.4(3)
Z	8	8	4	4
$F(000)$	2304	2176	504	568
$D_{calc.}$ (g cm^{-3})	2.514	2.549	2.259	2.629
μ(Mo–K$_\alpha$) (mm^{-1})	5.11	5.20	6.43	14.18
Structure determination				
Crystal size (mm)	$0.25\times0.15\times0.15$	$0.25\times0.25\times0.07$	$0.30\times0.25\times0.10$	$0.30\times0.22\times0.08$
Reflections measured	$\pm h,\pm k,\pm l$	$\pm h,\pm k,\pm l$	$+h,+k,\pm l$	$+h,+k,\pm l$
No. of reflections collected	6582	5352	1428	2965
No. of unique reflections	3394	2738	1329	1574
No. of observed reflections[b]	2395	1900	719	805
No. of parameters	149	157	82	81
R_{int}	0.0176	0.0233	0.0687	0.0621
R[b]	0.0327	0.0227	0.0962	0.0365
wR_2[b]	0.0730	0.0479	0.2380	0.1134
R (all data)	0.0433	0.0329	0.1457	0.0675
wR_2 (all data)	0.0739	0.0479	0.2604	0.1312
Weighting scheme, m[c]	0.0200	0.0000	0.1433	0.2728
Goodness-of-fit	1.213	0.776	1.724	0.618
Ratio of maximum least-squares shift to error	0.00	0.00	0.04	0.00
Maximum and minimum heights in final difference Fourier synthesis (e Å^{-3})	1.55, −0.82	0.49, −0.57	3.94, −0.92	1.77, −0.87
Extinction correction, ε	$1.2(4)\times10^{-4}$	$1.5(3)\times10^{-4}$	0.0	$5(1)\times10^{-3}$

[a] Common data for **5**, **6**, **8**, and **10**: T, 298 K; 2θ range 5–60°; oscillation angle ϖ, 1.0°.
[b] $F_o > 4\sigma(F_o)$.
[c] The weighting scheme: $w = [\sigma(F_o^2)+(mP)^2]^{-1}$, where $P = \max[(F_o^2, 0)+2F_c^2]/3$.

2.5. X-ray crystallography

Diffraction data for **5**, **6**, **8**, and **10** were collected on a Nonius kappa CCD diffractometer at 293 K using graphite monochromated Mo–K$_\alpha$ radiation ($\lambda = 0.71073$ Å) by recording 360 frames via ω-rotation ($\Delta\omega = 1°$; two times 10–20 s per frame). Crystal data and the details of the structure determination are shown in Table 1. The reflection data were corrected for Lorentz and polarization effects. No absorption correction was applied for the net intensities.

All structures were solved by direct methods using SHELXS-86 [21] and refined using SHELXL-93 [22]. After the full-matrix least-squares refinement of the non-hydrogen atoms with anisotropic thermal parameters the hydrogen atoms were placed in calculated positions in the aromatic rings (C–H = 0.93 Å) and in the methyl groups (C–H = 0.96 Å). In the final refinement the hydrogen atoms were riding with the carbon atom they were bonded to. The isotropic thermal parameters of the thienyl and furyl hydrogen atoms were fixed at 1.2 times to that of the corresponding carbon atom. The isotropic thermal parameters of the methyl hydrogen atoms were fixed at 1.5 times to that of the corresponding carbon atom. The scattering factors for the neutral atoms were those incorporated with the programs. Fractional coordinates and equivalent thermal parameters for the four complexes **5**, **6**, **8**, and **10** are given in Table 2.

Table 2
Fractional coordinates of non-hydrogen atoms of **5**, **6**, **8**, and **10**

	x	y	z	U_{eq}
$[PdCl_2\{(C_4H_3S)TeCH_3\}_2]$ (**5**)				
Pd	0.17208(2)	0.23367(3)	−0.07477(4)	0.0490(1)
Te(1)	0.15901(2)	0.09563(3)	0.05969(4)	0.0569(1)
Te(2)	0.18511(2)	0.35173(3)	0.11209(4)	0.0561(1)
Cl(1)	0.18556(7)	0.3444(1)	−0.2218(1)	0.0636(4)
Cl(2)	0.15397(9)	0.1118(1)	−0.2336(2)	0.0783(5)
S(1)	0.0740(1)	0.1472(2)	0.2326(2)	0.0927(6)
S(2)	0.0362(1)	0.3256(2)	−0.0796(3)	0.1240(8)
C(11)	0.1038(5)	0.1800(5)	0.3945(8)	0.094(2)
C(12)	0.1649(4)	0.1877(5)	0.4478(7)	0.087(2)
C(13)	0.1928(3)	0.1673(3)	0.3585(6)	0.054(1)
C(14)	0.1446(3)	0.1451(3)	0.2283(6)	0.056(1)
C(15)	0.0641(3)	0.0629(5)	−0.0529(7)	0.087(2)
C(21)	−0.0213(4)	0.3556(6)	−0.0384(10)	0.111(3)
C(22)	−0.0015(5)	0.3943(7)	0.0823(11)	0.128(3)
C(23)	0.0631(3)	0.4020(5)	0.1558(7)	0.072(2)
C(24)	0.0904(2)	0.3645(2)	0.0660(4)	0.064(2)
C(25)	0.1899(2)	0.4832(2)	0.0270(4)	0.086(2)
$[PdCl_2\{(C_4H_3O)TeCH_3\}_2]$ (**6**)				
Pd	0.17220(2)	0.23502(2)	−0.07929(3)	0.0433(1)
Te(1)	0.15687(2)	0.09716(2)	0.05945(3)	0.0520(1)
Te(2)	0.18068(2)	0.36229(2)	0.09987(3)	0.0524(1)
Cl(1)	0.18719(6)	0.34381(8)	−0.23279(11)	0.0560(3)
Cl(2)	0.15532(7)	0.10403(9)	−0.23247(12)	0.0688(4)
O(1)	0.0861(2)	0.1439(3)	0.2284(4)	0.078(1)
O(2)	0.0408(2)	0.3479(5)	−0.0759(5)	0.152(2)
C(11)	0.0925(4)	0.1721(4)	0.3577(6)	0.086(2)
C(12)	0.1505(4)	0.1957(4)	0.4335(6)	0.084(2)
C(13)	0.1857(3)	0.1801(4)	0.3546(5)	0.070(1)
C(14)	0.1443(2)	0.1514(3)	0.2314(5)	0.054(1)
C(15)	0.0579(2)	0.0735(4)	−0.0566(5)	0.090(2)
C(21)	−0.0169(4)	0.3516(7)	−0.0692(11)	0.152(4)
C(22)	−0.0103(4)	0.3740(6)	0.0486(10)	0.124(3)
C(23)	0.0558(4)	0.3842(5)	0.1309(7)	0.102(2)
C(24)	0.0843(2)	0.3660(4)	0.0530(5)	0.059(1)
C(25)	0.1801(3)	0.4952(3)	0.0002(5)	0.073(1)
$[PdCl_2\{(C_4H_3S)SeCH_3\}_2]$ (**8**)				
Pd	0.00000	0.00000	0.00000	0.0366(7)
Se	0.1153(3)	0.322(4)	0.0781(1)	0.0412(7)
Cl	0.2416(8)	−0.0449(11)	−0.0630(3)	0.057(2)
S	0.2972(12)	−0.0909(12)	0.1717(4)	0.078(2)
C(1)	0.326(4)	−0.085(5)	0.264(1)	0.082(5)
C(2)	0.255(4)	0.093(5)	0.298(1)	0.066(7)
C(3)	0.171(2)	0.258(3)	0.243(1)	0.034(4)
C(4)	0.191(2)	0.169(3)	0.170(1)	0.040(5)
C(5)	0.338(3)	0.410(4)	0.050(1)	0.065(7)
$[PtCl_2\{(C_4H_3S)SeCH_3\}_2]$ (**10**)				
Pt	0.00000	0.00000	0.00000	0.0478(3)
Se	0.1109(2)	0.3184(2)	0.07898(6)	0.0525(4)
Cl	0.2479(5)	−0.0412(6)	−0.0620(2)	0.0699(9)
S	0.2959(7)	−0.0916(7)	0.1723(2)	0.087(1)
C(1)	0.321(2)	−0.099(3)	0.2660(8)	0.082(4)
C(2)	0.254(2)	0.092(3)	0.2981(8)	0.073(4)
C(3)	0.173(1)	0.261(2)	0.2447(6)	0.050(3)
C(4)	0.191(2)	0.162(2)	0.1699(6)	0.058(3)
C(5)	0.340(2)	0.407(2)	0.0489(7)	0.066(4)

Table 3
^{77}Se-, ^{125}Te-, and ^{13}C-NMR spectroscopic data of the ligands and complexes

Compound	δ (^{77}Se)	δ (^{125}Te)	δ (^{13}C)				
			C(1)	C(2)	C(3)	C(4)	C(5)
$(C_4H_3S)TeCH_3$ (**1**)		218	140	129	134	98	−13
$[PdCl_2\{(C_4H_3S)TeCH_3\}_2]$ (**5**)		421, 429	139	129	134	106	4
$[PtCl_2\{(C_4H_3S)TeCH_3\}_2]$ (**7**)		[b]	139	129	134	101[c]	−5[c]
$(C_4H_3O)TeCH_3$ (**2**)		195	148	112	126	118	−15
$[PdCl_2\{(C_4H_3O)TeCH_3\}_2]$ (**6**)		409, 414	149	112	124	121	−3
$(C_4H_3S)SeCH_3$ (**3**)	133		134	128	130	125	12
$[PdCl_2\{(C_4H_3S)SeCH_3\}_2]$ (**8**)	233		135	128	132	123	18
$[PtCl_2\{(C_4H_3S)SeCH_3\}_2]$ (**10**)	233[a]		134	128	132	122	18
$(C_4H_3O)SeCH_3$ (**4**)	121		145	112	117	140	9
$[PdCl_2\{(C_4H_3O)SeCH_3\}_2]$ (**9**)	232		146	112	119	134	15

The numbering of carbon atoms follows the scheme indicated in Fig. 2.
[a] J_{Pt-Se}, 450 Hz.
[b] Not detected.
[c] Broad weak resonance.

3. Results and discussion

3.1. General

The reaction of $[MCl_2(PhCN)_2]$ (M = Pd, Pt) and $(C_4H_3E)E'Me$ (E = O, S; E′ = Se, Te) produces $[MCl_2\{(C_4H_3E)E'Me\}_2]$ with moderate to good yields. The complexes are air-stable and they are soluble in most organic solvents. With the exceptions of $[PtCl_2\{(C_4H_3S)TeMe\}_2]$ (**7**) and $[PdCl_2\{(C_4H_3O)SeMe\}_2]$ (**9**) for which only microcrystalline material was obtained, X-ray quality single crystals were grown from chloroform (**5** and **6**) or acetone (**8** and **10**). In the case of $[PdCl_2\{(C_4H_3S)SeMe\}_2]$ (**8**) twinning interfered with the structure determination. It was, however, possible to resolve the twinning and to establish the structure of **8** at a reasonable level of reliability. The largest peaks in the final difference Fourier map of this complex showed a weak shadow coordination polyhedron around palladium originating from the minor component in the twinned crystal.

3.2. NMR spectroscopy

The ^{13}C-, ^{77}Se-, and ^{125}Te-NMR spectra of the free ligands and their palladium and platinum complexes are shown in Table 3. Both the ^{77}Se and ^{125}Te resonances are shifted downfield upon the complex formation, as expected due to the decreasing shielding of the chalcogen atom. The values of the chemical shifts are quite typical for selane and tellurane ligands containing one alkyl and one aryl substituent [8]. It has been demonstrated that for analogous tellurium and selenium compounds the ^{125}Te and ^{77}Se chemical shifts show an constant ratio of ca. 1.6–1.8 [23–25]. Kemmitt et al. [14] have deduced that in metal complexes containing ligands with tellurium and selenium donor atoms the range in the δ(Te):δ(Se) ratio is 1.66–2.11 with an average of 1.8. In the present work we found the ratio to be 1.61–1.64 for the ligands and ca. 1.8 for the metal complexes (see Table 3).

Whereas both $[PdCl_2\{(C_4H_3S)TeMe\}_2]$ (**5**) and $[PdCl_2\{(C_4H_3O)TeMe\}_2]$ (**6**) exhibit two close-lying ^{125}Te resonances, the complexes with selenoether ligands (**8**–**10**) show only one ^{77}Se resonance. It indicates that while both **5** and **6** exist in solution as *cis* and *trans* isomers, there is only one isomer present in the case of **8**–**10**. The stereochemistry of $[ML_2X_2]$ (M = Pd, Pt; X = halide, L = R_2Se, R_2Te) complexes has been extensively investigated by NMR spectroscopy [4]. In many complexes both *cis* and *trans* isomers are indeed found in solution, as deduced by the presence of two Se or Te resonances with a small difference in chemical shifts ($\leq$ 30 ppm) [8,9]. It has been suggested that in solution the *trans*-isomers dominate and the tendency toward forming the *trans*-isomer is of the order Pd > Pt for the metal ion, Te > Se > S for the donor atom, and I > Br > Cl for the halido-ligand [1,4]. This has been discussed, both in terms of the thermodynamic and kinetic factors and attributed to the relative magnitude of the *trans*-influence of the seleno- and telluroether ligands [26]. It has also been reported that the ^{125}Te chemical shift of the *cis*-isomer lies at lower frequency to that of the *trans*-isomer [8]. Therefore the two resonances of **5** at 421 and 429 ppm and those of **6** at 409 and 414 ppm can be assigned to *cis*- and *trans*-isomers, respectively. In both cases this assignment leads to the *cis*/*trans* ratio of ca. 1.25.

It should be noted that we were unable to obtain the ^{125}Te-NMR spectrum for $[PtCl_2\{(C_4H_3S)TeMe\}_2]$ (**7**).

Furthermore, the resonances due to the two carbon atoms bound to tellurium appeared only as broad weak lines (see Table 3). These observations may be attributable to an exchange of the free and coordinated ligands that takes place at the NMR time scale.

The ^{13}C chemical shifts of all species shown in Table 3 are typical for the organic substituents in question in **5**–**10** [8,27]. The methyl carbon resonances of the free $(C_4H_3S)TeMe$ and $(C_4H_3O)TeMe$ ligands lie at -13.0 and -15.0 ppm, respectively, and those of $(C_4H_3S)SeMe$ and $(C_4H_3O)SeMe$ lie at 12.0 and 9.0 ppm, respectively. The thienyl and furyl carbons are found in the range 97.8–148.2 ppm. Upon complexation the methyl carbon resonances are shifted downfield. With the exception of C(4) the thienyl and furyl carbons are relatively stationary. The shift in C(4) depends on the nature of the chalcogen atom bound to the five-membered ring (see Table 3).

3.3. Molecular structures

The two tellurane complexes (**5** and **6**) are isomorphous as are the two selane complexes (**8** and **10**). The molecular structures of the two series of complexes as well as the numbering of the atoms are shown in Figs. 1 and 2. Selected bond lengths and angles are listed in Table 4 for **5** and **6**, and in Table 5 for **8** and **10**.

The two $[PdCl_2\{(C_4H_3E)TeMe\}_2]$ (E = S, O) complexes (**5** and **6**) have both crystallized in the *cis*-form. The palladium atom in both complexes exhibits approximately square planar coordination (see Table 4). The two Pd–Te bonds [Pd–Te(1) and Pd–Te(2)] are approximately normal to the planes defined by the donor atom and its two nearest neighbors [C(14)–Te(1)–C(15) and C(24)–Te(2)–C(25), respectively]. This implies that the tellurium atom is coordinated to palladium by involving mainly its 5*p*-lone pair orbital. The Pd–Te(1) and Pd–Te(2) bond distances in **5** are 2.538 and 2.546 Å, respectively. In **6** the corresponding Pd–Te(1) and Pd–Te(2) distances are somewhat shorter (both are 2.530 Å). These values can be compared and contrasted with 2.518 and 2.526 Å observed for *cis*-$[PdCl_2\{meso\text{-}(4\text{-}MeOC_6H_4Te)_2CH_2\}_2]$ [18], 2.525 and 2.528 Å observed for *cis*-$[PdBr_2\{meso\text{-}PhTe(CH_2)_3TePh\}_2]$ [14], and 2.625 and 2.653 Å observed for *cis*-$[Pd\{meso\text{-}(4\text{-}MeOC_6H_4Te)_2CH_2\}(Ph_2PCH_2CH_2PPh_2)](ClO_4)_2\cdot 4H_2O$ [18]. The Pd–Te bond lengths in *trans*-$[PdCl_2\{Te(CH_2)_4\}_2]$ and *trans*-$[Pd(SCN)_2\{Te(CH_2)_3SiMe_3\}_2]$ are 2.593 Å [16] and 2.606 Å [12], respectively. It is also worth noting that the four terminal Pd–Te bonds that are in the *trans*-positions to the bridging tellurium atoms in the tetrameric complex $[\{PdI(o\text{-}C_6H_4(TeMe)Te\}_4]$ span a narrow range 2.540–2.554 Å [15].

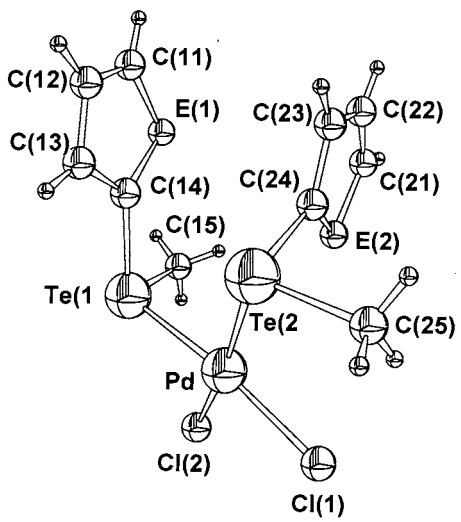

Fig. 1. The molecular structure of $[PdCl_2\{(C_4H_3S)TeMe\}_2]$ (**5**) and $[PdCl_2\{(C_4H_3O)TeMe\}_2]$ (**6**) indicating the numbering of the atoms. The thermal ellipsoids have been drawn at 50% probability.

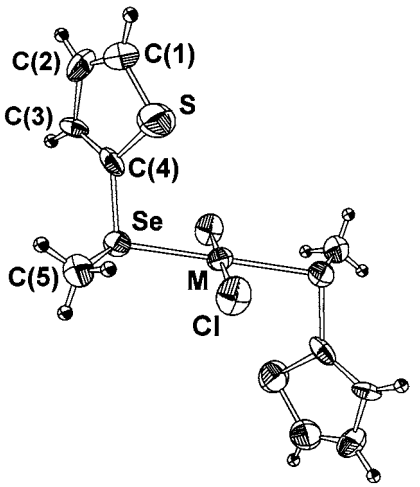

Fig. 2. The molecular structure of $[PdCl_2\{(C_4H_3S)SeMe\}_2]$ (**8**) and $[PtCl_2\{(C_4H_3S)SeMe\}_2]$ (**10**) indicating the numbering of the atoms. The thermal ellipsoids have been drawn at 50% probability.

The relative magnitudes of the Pd–Te bond lengths can be rationalized in terms of the relative *trans*-influence of the ligands [1,18]. The longer Pd–Te bonds in *cis*-$[Pd\{meso\text{-}(4\text{-}MeOC_6H_4Te)_2CH_2\}(Ph_2PCH_2CH_2PPh_2)](ClO_4)_2\cdot 4H_2O$ [18] than in **5**, **6**, *cis*-$[PdCl_2\{meso\text{-}(4\text{-}MeOC_6H_4Te)_2CH_2\}_2]$ [18] and *cis*-$[PdBr_2\{meso\text{-}PhTe(CH_2)_3TePh\}_2]$ [14] indicate that the phosphorus donor shows a stronger *trans*-influence than the halogen donor. The *trans*-complexes *trans*-$[PdCl_2\{Te(CH_2)_4\}_2]$ [16] and *trans*-$[Pd(SCN)_2\{Te(CH_2)_3SiMe_3\}_2]$ [12] show rather long Pd–Te bonds consistent with the suggestion that the *trans*-influence of tellurium is comparable to that of sulfur [18].

The Pd–Cl(1) and Pd–Cl(2) distances in **5** are 2.351 and 2.352 Å, respectively, and the corrsponding dis-

tances in **6** are somewhat longer (2.356 and 2.359 Å, respectively). The Pd–Cl distances in *cis*-[$PdCl_2${*meso*-(4-$MeOC_6H_4Te)_2CH_2$}$_2$] are 2.39 and 2.42 Å [18], and in *trans*-[$PdCl_2${$Te(CH_2)_4$}$_2$] 2.319 and 2.326 Å [14]. The differences in the *cis*- and *trans*-isomers can again be explained in terms of the relative *trans*-influence.

There is a long-standing debate whether back-donation of π-electron density from palladium or platinum to the Group 16 donor atom can take place [1–4]. The suggestion of the double bond character in the M–E bond (M = Pd, Pt; E = S, Se,Te) was based on the observation that the bonds were shorter than the sums of the covalent radii of the pertinent elements. The scattered nature of the structural data has eluded more exact inferences, but there is a general consensus that the back donation from palladium or platinum to the chalcogen donors is in any case very small being negligible for sulfur and selenium [1–4]. Only in the case of tellurium may a small effect be observed.

Table 4
Selected bond lengths (Å) and angles (°) for [$PdCl_2${$(C_4H_3E)TeCH_3$}$_2$] [E = S (**5**), E = O (**6**)]

	5	**6**
Bond length (Å)		
Pd–Te(1)	2.538(1)	2.530(1)
Pd–Te(2)	2.546(1)	2.530(1)
Pd–Cl(1)	2.351(1)	2.356(1)
Pd–Cl(2)	2.352(1)	2.359(1)
Te(1)–C(14)	2.107(6)	2.113(5)
Te(1)–C(15)	2.122(6)	2.128(5)
Te(2)–C(24)	2.096(4)	2.082(5)
Te(2)–C(25)	2.109(4)	2.122(5)
E(1)–C(11)	1.661(8)	1.379(6)
E(1)–C(14)	1.693(6)	1.346(5)
C(11)–C(12)	1.324(10)	1.287(7)
C(12)–C(13)	1.407(9)	1.417(7)
C(13)–C(14)	1.436(8)	1.318(6)
E(2)–C(21)	1.654(9)	1.375(9)
E(2)–C(24)	1.665(4)	1.341(6)
C(21)–C(22)	1.312(11)	1.240(10)
C(22)–C(23)	1.411(11)	1.420(10)
C(23)–C(24)	1.470(8)	1.287(7)
Bond angles (°)		
Te(1)–Pd–Te(2)	93.54(2)	93.90(2)
Te(1)–Pd–Cl(1)	171.32(4)	170.74(3)
Te(1)–Pd–Cl(2)	79.49(4)	78.59(3)
Te(2)–Pd–Cl(1)	94.99(4)	95.30(3)
Te(2)–Pd–Cl(2)	172.55(4)	171.58(3)
Cl(1)–Pd–Cl(2)	92.09(6)	92.30(4)
C(14)–Te(1)–C(15)	93.4(2)	92.6(2)
C(24)–Te(2)–C(25)	93.6(1)	94.7(2)
Pd–Te(1)–C(14)	109.7(1)	110.2(1)
Pd–Te(1)–C(15)	101.0(2)	99.3(1)
Pd–Te(2)–C(24)	95.7(1)	96.0(1)
Pd–Te(2)–C(25)	104.6(1)	104.0(1)
C(11)–E(1)–C(14)	92.2(4)	105.8(4)
E(1)–C(11)–C(12)	113.3(6)	109.9(5)
C(11)–C(12)–C(13)	115.0(7)	107.7(5)
C(12)–C(13)–C(14)	108.0(6)	106.0(5)
C(13)–C(14)–E(1)	111.4(4)	110.5(4)
C(21)–E(2)–C(24)	93.5(4)	105.7(6)
E(2)–C(21)–C(22)	112.3(7)	110.9(8)
C(21)–C(22)–C(23)	117.0(8)	106.7(7)
C(22)–C(23)–C(24)	105.7(4)	107.6(6)
C(23)–C(24)–E(2)	111.4(1)	109.0(5)

Table 5
Selected bond lengths (Å) and angles (°) for [MCl_2{$(C_4H_3S)SeCH_3$}$_2$] [M = Pd (**8**), M = Pt (**10**)]

	8	**10**
Bond length (Å)		
M–Se	2.439(2)	2.411(4)
M–Cl	2.263(6)	2.310(1)
Se–C(1)	1.91(2)	1.89(1)
Se–C(5)	1.88(3)	1.97(1)
S–C(1)	1.71(2)	1.67(1)
S–C(4)	1.65(2)	1.68(1)
C(1)–C(2)	1.42(3)	1.48(2)
C(2)–C(3)	1.47(3)	1.49(2)
C(3)–C(4)	1.33(4)	1.38(2)
Bond angles (°)		
Se–M–Cl	96.3(2)	95.85(9)
C(1)–Se–C(5)	99.0(9)	98.0(5)
M–Se–C(1)	101.5(6)	101.4(4)
M–Se–C(5)	109.3(7)	107.9(4)
C(1)–S–C(4)	90.7(14)	93.5(7)
S–C(1)–C(2)	113.7(15)	114.9(9)
C(1)–C(2)–C(3)	107.1(19)	104.2(11)
C(2)–C(3)–C(4)	112.0(20)	114.9(12)
C(3)–C(4)–S	116.4(12)	112.5(11)

The comparison of the relative bond lengths in **5**, **6**, and *cis*-[$PdCl_2${*meso*-(4-$MeOC_6H_4Te)_2CH_2$}$_2$] enables some further inferences to be made. All three complexes contain two Pd–Te bonds and two Pd–Cl bonds in *cis*-positions. The effects due to the differences in the *trans*-influence are thus minimized in these complexes. The average lengths of the relevant bonds in these three complexes are given in Table 6.

The Pd–Te bond lengths increase in the order *cis*-[$PdCl_2${*meso*-(4-$MeOC_6H_4Te)_2CH_2$}$_2$] < **6** < **5**. This order in the bond lengths can be explained by a slight increase of back donation and thus π-electron density as a consequence of the increasing electron-withdrawing nature of the substituent in tellurium[1]. The opposite trend in the lengths of the Pd–Cl bonds that is apparent in Table 6 is also consistent with the concept of increasing back donation as the electron withdrawing nature of the tellurium-containing ligand increases.

It has been suggested [4] that the acceptor orbital of the tellurane ligand for the back donation from the metal is more likely to be an antibonding Te–C σ* orbital than the empty 5d-orbital of tellurium that is expected to lie at a rather high energy. Thus the

[1] It is to be expected that furyl is more electrophilic than thienyl because oxygen is more electronegative than sulfur.

Table 6
The average Pd–Te, Pd–Cl, Te–C(alkyl), and Te–C(aryl) bond lengths (Å) in *cis*-[$PdCl_2${*meso*-(4-$MeOC_6H_4Te)_2CH_2$}$_2$], **6**, and **5**

Complex	Pd–Te	Pd–Cl	Te–C(alkyl)	Te–C(aryl)
Cis-[$PdCl_2${*meso*-(4-$MeOC_6H_4Te)_2CH_2$}$_2$][a]	2.52	2.40	—	2.12
[$PdCl_2${$(C_4H_3O)TeMe$}$_2$] (**6**)	2.53	2.36	2.13	2.10
[$PdCl_2${$(C_4H_3S)TeMe$}$_2$] (**5**)	2.54	2.35	2.12	2.10

[a] See Drake et al. [18].

strengthening of the π-bond as a consequence of back bonding introduces electron density into the antibonding orbitals of the Te-C bonds and should therefore render these bonds longer. The stronger the $d\pi$-σ*(Te–C) interaction, the longer the Te–C bonds. Since it is to be expected that the Te–C(alkyl) and Te–C(aryl) bonds are of different lengths with the latter shorter, the trends in these bond lengths are explored separately. The relative lengths of these bonds are also consistent with the concept of back donation even though the effect is very small (see Table 6).

The two [MCl_2{$(C_4H_3S)SeMe$}$_2$] (M = Pd, Pt) complexes (**8** and **10**) are both found in the *trans*-form. It can be seen from Table 5 that, like in the case of **5** and **6**, the coordination around the metal atoms is a slightly distorted square plane in both cases. The M–Se distances are 2.439 and 2.411 Å and the M–Cl distances are 2.263 and 2.310 Å for the palladium (**8**) and platinum (**10**) complex, respectively. They can be compared with 2.429 and 2.295 Å observed for the Pd–Se and Pd–Cl distances in [$PdCl_2(Me_3SiCH_2SeMe)_2$], and with 2.418 and 2.305 Å observed for the Pt–Se and Pt–Cl distances in [$PtCl_2(Me_3GeCH_2SeMe)_2$] [13]. The Pd–Se distance in [$PdCl_2(Et_2Se)_2$] is 2.424 Å and the Pd–Cl distance is 2.268 Å [11]. It is interesting to note that the Pd–Cl distances in all *trans*-complexes are shorter than in the *cis*-complexes discussed above. This is consistent with the stronger *trans*-influence of the chalcogen atoms compared to the halogen atoms. The Pd–Se and Pt–Se bonds are close to the single bond lengths and therefore the back donation from the metal to selenium is not significant.

3.4. Packing

The complexes **5** and **6** form dimers with short palladium–palladium contacts, as shown in Fig. 3. In **5** the closest Pd···Pd contact is 3.399(1) and in **6** 3.307(1) Å. This pairing up of two square planar complexes is quite common for all mononuclear [ML_2X_2] complexes with tellurium-containing ligands as also indicated in Fig. 3. In *cis*-[$PdCl_2${*meso*-(4-$MeOC_6H_4Te)_2CH_2$}$_2$] the Pd···Pd distance is 3.242 Å [18], in *cis*-[$PdBr_2${*meso*-$PhTe(CH_2)_3TePh$}$_2$] 3.568 Å [14] and in *trans*-[$PtI_2(PhTeMe)_2$] 3.332 Å [17]. All these distances, however, are longer than the sum of the van der Waals' radii for two palladium or platinum atoms (2.76 Å for both elements [28]) and therefore the dimer formation is not a consequence of metal–metal interaction.

It can be seen from Fig. 3 that the pairing of the complexes is a consequence of the attractive interactions between the halogen ligand in one complex and the three-coordinated tellurium in the other. In **5** the chlorine–tellurium distances Te(1)···Cl(1) and Te(2)···Cl(2) are 3.472 and 3.523 Å, respectively. In **6** the correponding distances are 3.401 and 3.494 Å and in *cis*-[$PdCl_2${*meso*-(4-$MeOC_6H_4Te)_2CH_2$}$_2$] 3.393 and 3.520 Å [18]. These distances are significantly shorter than the sum of van der Waals' radii between chlorine

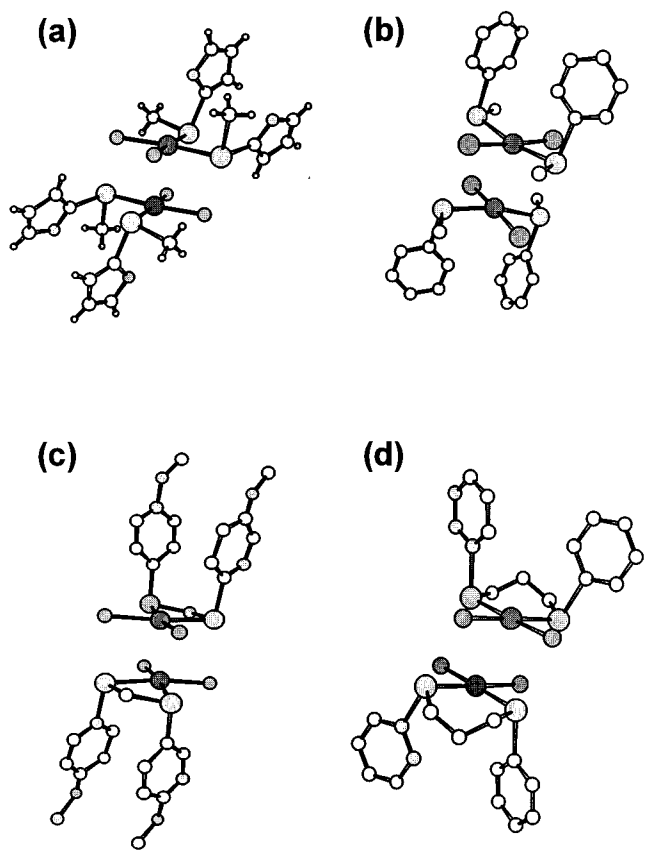

Fig. 3. The dimer formation in [MX_2L_2] (L = tellurium-containing ligand, X = halogen). (a) *Cis*-[$PdCl_2${C_4H_3E)TeMe$}$_2$] (E = S, O) (**5** and **6**); (b) *trans*-[$PtI_2(PhTeMe)_2$] 3.332 Å (redrawn from crystal data given in Ref. [17]); (c) *cis*-[$PdCl_2${*meso*-(4-$MeOC_6H_4Te)_2CH_2$}$_2$] (redrawn from crystal data given in Ref. [18]); and (d) *cis*-[$PdBr_2${*meso*-$PhTe(CH_2)_3TePh$}$_2$] (redrawn from crystal data given in Ref. [14]).

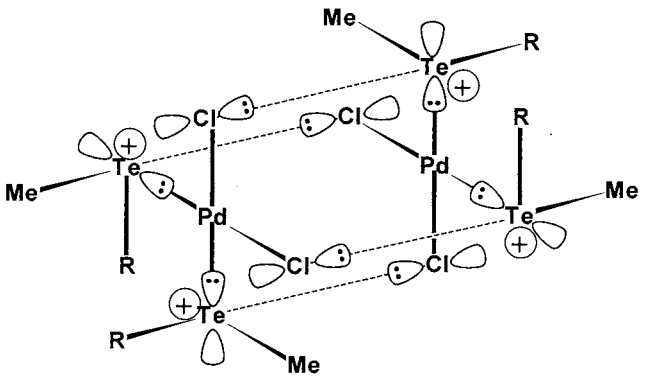

Fig. 4. The chlorine–tellurium interaction in the dimer-formation of *cis*-[$PdCl_2\{C_4H_3E)TeMe\}_2$] (**5** and **6**).

and tellurium (4.01 Å [28]). The Te···Br contacts of 3.623 and 3.647 Å in *cis*-[$PdBr_2\{$*meso*-$PhTe(CH_2)_3TePh\}_2$] [14], and the Te···I contacts of 3.679 and 3.862 Å in *trans*-[$PtI_2(PhTeMe)_2$] [17] are also significantly shorter than the sums of the respective van der Waals' radii (Te···Br 4.15 Å; Te···I 4.35 Å [28]). Atomic coordinates are not reported for *trans*-[$PdCl_2\{Te(CH_2)_4\}_2$] [16] and it is therefore not possible to judge whether this

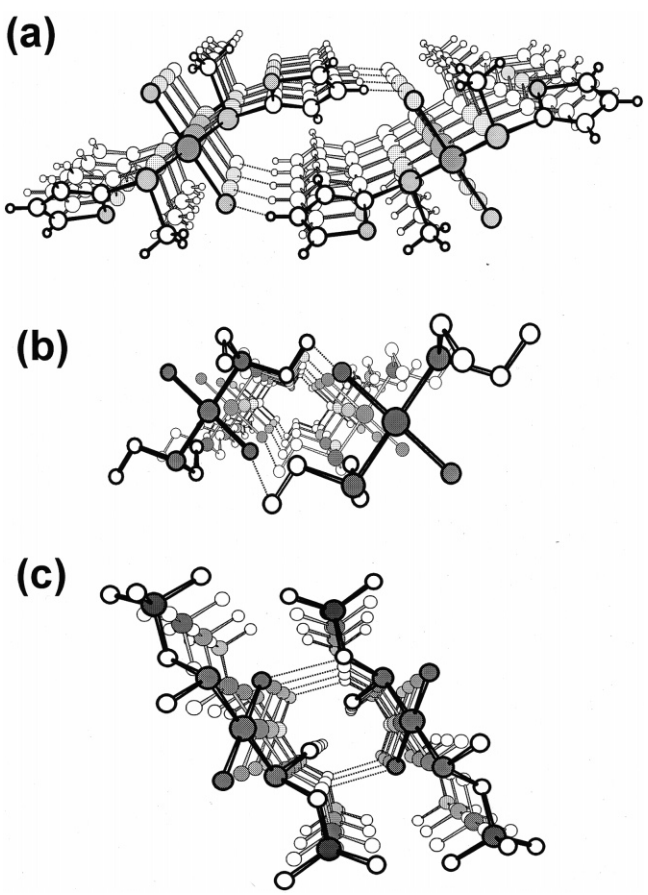

Fig. 5. The stack-formation in (a) *trans*-[$MCl_2\{C_4H_3S)SeMe\}_2$] (M = Pd, Pt) (**8** and **10**); (b) *trans*-[$PdCl_2(Et_2Se)_2$] (redrawn from crystal data given in Ref. [11]); and (c) *trans*-[$MCl_2(Me_3QCH_2SeMe)_2$] (M = Pd, Pt; Q = Si, Ge) (redrawn from crystal data given in Ref. [13]).

complex also forms a similar dimer. Both telluracyclopentane ligands, however, are folded on the same side of the square plane. This strongly suggests a dimeric configuration with chlorine–tellurium close contacts.

The nature of the interaction is exemplified in Fig. 4 for **5** and **6**, though the same arguments can be applied for other complexes that have been reported previously [14,17,18]. The three-coordinated tellurium is expected to carry a significant positive charge. It therefore attracts the *p*-lone-pair of the halogen ligand from the neighboring complex. The shorter Te···Cl contacts in **6** than in **5** can be explained by the more electron-withdrawing nature of the furyl ring compared to the thienyl ring that renders tellurium more positively charged in **6** than in **5**. The even shorter Te···Cl contact in *cis*-[$PdCl_2\{$*meso*-$(4\text{-}MeOC_6H_4Te)_2CH_2\}_2$] also agrees well with this concept.

The packing in selenoether palladium (**8**) or platinum (**10**) complexes is substantially different from that in telluroether complexes as shown in Fig. 5. The complexes are stacked together into infinite skewed columns. There are no Cl···Se close contacts within the columns, but there are Cl···H(2)–C(2) interactions between the columns (the Cl···C(2) distance is 3.614 and 3.601 Å for **8** and **10**, respectively). The arrangement implies weak hydrogen bonds between the columns. They tie the complexes in two adjacent stacks together to form a infinite helix (see Fig. 5). The same kind of helical stacking configuration is also observed in *trans*-[$PdCl_2(Et_2Se)_2$] (Cl···C 3.833 Å) [11], and *trans*-[$MCl_2(Me_3QCH_2SeMe)_2$] (M = Pd, Pt; Q = Si, Ge) (Cl···C 3.690 Å) [13] as also shown in Fig. 5.

The differences in the packing of the telluroether and selenoether complexes are probably explained by the smaller electronegativity of tellurium compared to that of selenium. Tellurium is more easily polarized and the three-coordinated atom carries a larger positive charge than the three-coordinated selenium atom and therefore is more strongly attracted by halogen atoms.

4. Supplementary material available

Lists of anisotropic thermal parameters, calculated hydrogen atom coordinates, complete bond distances and angles, and structure factors for complexes **5**, **6**, **8**, and **10** are available from the authors upon request.

Acknowledgements

Financial support from Neste Oy Foundation, Academy of Finland, and Alfred Kordelin Foundation is gratefully acknowledged.

References

[1] S.G. Murray, F.R. Hartley, Chem. Rev. 81 (1981) 365.
[2] H.J. Gysling, Coord. Chem. Rev. 42 (1982) 133.
[3] H. Gysling, in: S. Patai, Z. Rappoport (Eds.), The Chemistry of Organic Selenium and Tellurium Compounds, vol. 1, Wiley, New York, 1986, p. 221.
[4] E.G. Hope, W. Levason, Coord. Chem. Rev. 122 (1993) 109.
[5] W. Levason, in: F.R. Hartley (Ed.), The Chemistry of Organophosphorus Compounds, vol. 1, Wiley, New York, 1990 Ch. 15.
[6] R.J. Angelici, Acc. Chem. Res. 21 (1988) 387.
[7] R.J. Angelici, Coord. Chem. Rev. 105 (1990) 61.
[8] T. Kemmit, W. Levason, Inorg. Chem. 29 (1990) 731.
[9] P.L. Goggin, R.J. Goodfellow, S.R. Haddock, J. Chem. Soc. Chem. Commun. (1975) 176.
[10] H.J. Gysling, N. Zumbulyadis, J.A. Robertson, J. Organomet. Chem. 209 (1981) C41.
[11] P.E. Skakke, S.E. Rasmussen, Acta Chem. Scand. 24 (1970) 2634.
[12] H.J. Gysling, H.R. Luss, D.L. Smith, Inorg. Chem. 18 (1979) 2696.
[13] R.K. Chadha, J.M. Chehayber, J.E. Drake, Inorg. Chem. 25 (1986) 611.
[14] T. Kemmitt, W. Levason, M. Webster, Inorg. Chem. 28 (1989) 692.
[15] T. Kemmitt, W. Levason, M.D. Spicer, M. Webster, Organometallics 9 (1990) 1181.
[16] T. Kemmitt, W. Levason, R.D. Oldroyd, M. Webster, Polyhedron 11 (1992) 2165.
[17] W. Levason, M. Webster, C.J. Mitchell, Acta Crystallogr. C48 (1992) 1931.
[18] J.E. Drake, J. Yang, A. Khalid, V. Srivastava, A.K. Singh, Inorg. Chim. Acta 254 (1997) 57.
[19] M.S. Kharasch, R.C. Seyler, F.R. Mayo, J. Am. Chem. Soc. 60 (1938) 882.
[20] L. Engman, M.P. Cava, Organometallics 1 (1982) 470.
[21] G.M. Sheldrick, SHELXS-86, Program for Crystal Structure Determination, University of Göttingen, 1986.
[22] G.M. Sheldrick, SHELXL-93, Program for Crystal Structure Refinement, University of Göttingen, 1993.
[23] H.C.E McFarlane, W. McFarlane, J. Chem. Soc. Dalton Trans. (1973) 2416.
[24] D.H. O'Brien, N. Dereu, C.K. Huang, K.J. Irgolic, Organometallics 2 (1983) 305.
[25] T. Chivers, R.S. Laitinen, K.J. Schmidt, J. Taavitsainen, Inorg. Chem. 32 (1993) 337.
[26] H. Schumann, A.A. Arif, A.L. Rheingold, C. Janiak, R. Hoffmann, N. Kuhn, Inorg. Chem. 30 (1991) 1618.
[27] S. Gronowitz, I. Johnson, A.B. Hörnfeldt, Chim. Scr. 7 (1975) 76.
[28] J. Emsley, The Elements, 2nd ed., Clarendon, Oxford, 1991.